Acta Biochim Biophys Sin 2022, 54(11): 1648–1657
https://doi.org/10.3724/abbs.2022158
Advance Access Publication Date: 2 November 2022
Original Article

Original Article

Neuregulin-1/ErbB4 upregulates acetylcholine receptors via Akt/mTOR/p70S6K: a study in a rat model of obstetric brachial plexus palsy and *in vitro*

Jing Qiao[1,2,3,†], Jiayu Sun[1,2,3,†], Liang Chen[1,2,3,*], Bo Li[4], and Yudong Gu[1,2,3]

[1]Department of Hand Surgery, Huashan Hospital and Institutes of Biomedical Sciences, Fudan University, Shanghai 200040, China, [2]Key Laboratory of Hand Reconstruction, Ministry of Health, Shanghai 200040, China, [3]Shanghai Key Laboratory of Peripheral Nerve and Microsurgery, Shanghai 200040, China, and [4]Department of Orthopedic Surgery, Yangpu Hospital, Tongji University, Shanghai 200090, China
[†]These authors contributed equally to this work.
*Correspondence address. Tel: +86-21-52888204; E-mail: liangchen1960@163.com

Received 20 February 2022 Accepted 26 April 2022

Abstract

In obstetric brachial plexus palsy (OBPP), the operative time window for nerve reconstruction of the intrinsic muscles of the hand (IMH) is much shorter than that of biceps. The reason is that the atrophy of IMH becomes irreversible more quickly than that of biceps. A previous study confirmed that the motor endplates of denervated intrinsic muscles of the forepaw (IMF) were destabilized, while those of denervated biceps remained intact. However, the specific molecular mechanism of regulating the self-repair of motor endplates is still unknown. In this study, we use a rat model of OBPP with right C5-C6 rupture plus C7-C8-T1 avulsion and left side as a control. Bilateral IMF and biceps are harvested at 5 weeks postinjury to assess relative protein and mRNA expression. We also use L6 skeletal myoblasts to verify the effects of signaling pathways regulating acetylcholine receptor (AChR) protein synthesis *in vitro*. The results show that in the OBPP rat model, the protein and mRNA expression levels of NRG-1/ErbB4 and phosphorylation of Akt/mTOR/p70S6K are lower in denervated IMF than in denervated biceps. In L6 myoblasts stimulated with NRG-1, overexpression and knockdown of ErbB4 lead to upregulation and downregulation of AChR subunit protein synthesis and Akt/mTOR/p70S6K phosphorylation, respectively. Inhibition of mTOR abolishes protein synthesis of AChR subunits elevated by NRG-1/ErbB4. Our findings suggest that in the OBPP rat model, lower expression of AChR subunits in the motor endplates of denervated IMF is associated with downregulation of NRG-1/ErbB4 and phosphorylation of Akt/mTOR/p70S6K. NRG-1/ErbB4 can promote protein synthesis of the AChR subunits in L6 myoblasts via phosphorylation of Akt/mTOR/p70S6K.

Key words acetylcholine receptor subunits, denervation, motor endplates, obstetric brachial plexus palsy

Introduction

Obstetric brachial plexus palsy (OBPP) is a brachial plexus traction injury of newborns during delivery resulted from a force separating the head and shoulders. Between 10% and 30% of OBPP patients experience permanent dysfunction and require nerve reconstruction to restore function [1]. For OBPP, it is clinically considered that the C8-T1 spinal nerve innervating the intrinsic muscle of the hand (IMH) should be reconstructed at most 3 months after birth [2]; however, with regard to the nerve reconstruction of C5-C6 innervated muscle in the upper arm, nerve grafting at 30 months after birth may still provide functional improvement [3]. Compared with the biceps, which is innervated by the upper trunk of the plexus, IMH is innervated by the lower trunk, and its atrophy becomes irreversible more quickly. In an OBPP rat model, we confirmed that when the brachial plexus was reconstructed 5 weeks after injury, atrophy of the intrinsic muscles of the forepaw (IMF) was irreversible, whereas atrophy of the biceps was still reversible [4]. Furthermore, by using the rat model, we found different expression profiles of miRNAs [5], mRNAs [6], and proteins [7] associated with the formation and functional regulation of neuromuscular junctions (NMJs) between denervated biceps and denervated IMF, indicating that self-repair of NMJs in denervated

biceps is more active than that in denervated IMF.

NMJs consist of terminal Schwann cells, axonal endings, a synaptic cleft, a postsynaptic membrane containing nicotinic acetylcholine receptors (AChRs), and a supportive sarcoplasm. NMJs in skeletal muscles of homothermal animals appear platy, so they are also known as motor endplates (MEPs). At the early stage after peripheral nerve transection, MEPs start to fragmentize, but AChRs can still regenerate at the original synapse for self-repair. If transected nerves can be repaired at this point, MEPs can still adopt regenerative axons [8]. When greatly fragmented or disappeared, MEPs have little potential for reinnervation [9]. In our previous study on an OBPP rat model, MEPs of denervated IMF were found to be destabilized, while those of denervated biceps remained stable, and AChR expression levels were lower in denervated IMF than in denervated biceps [10]. These results indicated that in OBPP, relatively worse self-repair of MEPs in denervated IMH was responsible for the fact that IMH atrophy became irreversible more rapidly. The specific molecular mechanisms regulating the self-repair of MEPs remain unknown, but they may become intervention targets for delaying irreversible atrophy after nerve transection.

Members of the ErbB family, including ErbB2, ErbB3, and ErbB4, are receptor tyrosine kinases mainly expressed at the postsynaptic membrane [11]. When combined with neuregulin-1 (NRG-1) secreted by motor neurons or Schwann cells, ErbB dimers can activate downstream signaling pathways, such as ERK/p38 MAPK and Akt/mTOR, thereby participating in the formation of MEPs [12,13]. In our previous pathway analysis of miRNA expression profiles in the OBPP rat model, microRNAs targeting the NRG-1/ErbB pathway, such as miR-221 and miR-222, were upregulated in denervated biceps but not regulated in denervated IMF at 5 weeks postinjury [5]. Downregulation of NRG-1/ErbB signaling in NMJs reduced AChR density and clustering at the postsynaptic membrane [14]. Therefore, NRG-1/ErbB4 might participate in the self-repair of MEPs by regulating AChR function at the postsynaptic membrane. However, specific regulatory mechanism of NRG-1/ErbB pathway on denervated skeletal muscles remains to be explored.

In this study, we investigated the expression of NRG-1/ErbB and phosphorylation of its downstream pathway Akt/mTOR/p70S6K in denervated IMF and denervated biceps in the OBPP rat model. Furthermore, we also verified the effects of both pathways on regulating AChR subunit protein synthesis in L6 rat skeletal myoblasts.

Materials and Methods

Ethics committee approval

Our animal experimental procedures were approved by the Animal Welfare and Ethics Committee, Department of Experimental Animal Science, Fudan University (No. 20161007A327) in March 2016. Experiments were performed in accordance with the Guide for the Care and Use of Laboratory Animals of the US National Institutes of Health (NIH, Bethesda, USA).

Development of the OBPP model and specimen collection

Sprague-Dawley rats (weighing 11–13 g, 7 days old) were purchased from the Experimental Animal Science Department of Fudan University (Shanghai, China). Before establishing the OBPP model, the rats were anesthetized intraperitoneally with 1% pentobarbital sodium at a dose of 5 mL/kg. Right C5–C6 spinal nerves were lacerated, and right C7–C8–T1 were avulsed at the same time. The left side of each rat was not damaged and was used as a normal control. The rats were sacrificed 5 weeks after surgery, and the bilateral IMF and biceps were collected to examine the morphology of MEPs by using a TCS SP8 microscope (Leica, Solms, Germany) and measure the relative expression levels of NRG-1, ErbB2, ErbB3, ErbB4, AChRα, AChRβ, AChRδ, Akt, phosphorylated Akt (p-Akt), mTOR, phosphorylated mTOR (p-mTOR), p70S6K, and phosphorylated p70S6K (p-p70S6K) by real-time PCR or western blot analysis.

Cell culture

L6 rat skeletal myoblasts were purchased from the National Collection of Authenticated Cell Cultures (Shanghai, China) and cultured in Dulbecco's modified Eagle's medium (DMEM) containing 1% penicillin and streptomycin (Gibco, Waltham, USA) and 10% fetal bovine serum (Gibco) at 37°C in 5% CO_2 (Thermo Scientific, Waltham, USA). L6 rat skeletal myoblasts from passages 2 to 5 were used in the experiment. During *in vitro* experiment, NRG-1 (200 ng/mL) was added to the medium all the time. In addition, to inhibit Akt, Erk, p38, or mTOR, L6 myoblasts were treated with 10 μM MK-2206 (inhibitor of Akt; Sigma, St Louis, USA), 10 μM PD98059 (inhibitor of Erk; Sigma), 10 μM SB203580 (inhibitor of p38; Sigma), 10 μM rapamycin (inhibitor of mTOR; Sigma), or vehicle as a control for 48 h.

Construction of plasmid and generation of overexpression cell lines

First, ErbB4 DNA was amplified by standard PCR from ErbB4 cDNA (FulenGen, Guangzhou, China) and cloned into PRK5 lentiviral vectors (Addgene, Watertown, USA) between the restriction enzyme cleavage sites *Bam*HI and *Eco*RI. After that, the ErbB4 recombinant plasmid was determined by Sanger sequencing and used to produce lentivirus. PRK5 plasmid without insertion of cDNA was used to produce a control lentiviral vector. To overexpress ErbB4 protein, L6 myoblasts were infected with 10^6 TU/mL lentivirus for 12 h. Then, the completed culture medium was added. To remove L6 myoblasts without ErbB4 protein overexpressing, puromycin (3 μg/mL) was added to the medium when L6 myoblasts were infected with lentivirus after 48 h. ErbB4-overexpressing L6 myoblast lines were generated when puromycin was maintained in the medium for two weeks.

Cell transfection

ErbB4-specific siRNA and negative control (NC) siRNA were purchased from GenePharma (Shanghai, China). The ErbB4 siRNA sequence was 5′-CCAGAACAAATTCCTATGTTA-3′, and the negative control sequence was 5′-UUCUCCGAACGUGUCACGUTT-3′. L6 myoblasts were transfected with ErbB4 siRNA to inhibit the endogenous ErbB4 level using Lipo2000 (Invitrogen) in accordance with the manufacturer's protocol, and NC siRNA transfection was used as a control. The medium was replaced by complete DMEM after 6 h of transfection, and RNA or protein was collected 48 h later to determine the transfection efficiency.

Immunofluorescence assay

IMF and biceps were fixed in 4% paraformaldehyde at 4°C overnight, followed by cryoprotection in 30% sucrose in phosphate-buffered saline (PBS) overnight. Afterwards, the IMF and biceps were embedded into Optimal Cutting Temperature Compound (OCT; Boster, Wuhan, China). The IMF and biceps were

cryosectioned to sections with a thickness of 20 μm. L6 myoblasts were fixed in 4% paraformaldehyde at 25°C for 15 min. Then, the sections or cells were first permeabilized with 0.3% Triton X-100 (Sigma-Aldrich, St Louis, USA) for 30 min, followed by incubation in blocking buffer (3% BSA; Sigma-Aldrich) for 1 h at 25°C. The sections were then incubated with anti-neurofilament heavy chain antibody (1:1000; Abcam, Eugene, USA), anti-ErbB4 antibody (1:50; GeneTex, Irvine, USA), and anti-p-mTOR (1:500; Cell Signaling Technology, Danvers, USA) at 4°C overnight. The sections were washed with PBS, followed by incubation with goat anti-mouse IgG H&L (Alexa Fluor 594) (1:1000; Invitrogen, Carlsbad, USA), α-bungarotoxin-ATTO-488 (1:100; Alomone Labs, Jerusalem, Israel) (for AChRs), or goat anti-rabbit IgG H&L (Alexa Fluor 633) (1:1000; Invitrogen) for 2 h at 25°C away from light. The sections were detected with a confocal microscope (TCS SP8; Leica, Wetzlar, Germany), and 5 fields were randomly selected from each section under the bright field.

Western blot analysis

The IMF and biceps in the rats and the L6 myoblasts were lysed in radioimmunoprecipitation assay cell lysis buffer (Beyotime Biotechnology, Haimen, China) containing protease and phosphatase cocktail inhibitors. The protein concentration was measured using a protein quantitative assay kit (Thermo Fisher). Equal amounts of protein extracts were resolved by sodium dodecyl sulfate-polyacrylamide gel electrophoresis (10% SDS-PAGE) and transferred to polyvinylidene fluoride (PVDF) membranes (Millipore, Bedford, USA). The PVDF membranes were blocked with 5% nonfat milk for 1 h at 25°C and then washed with Tris-buffered saline containing 0.1% Tween-20. The membranes were incubated with anti-AChRα antibody (1:1000; Abnova, Taipei, China), anti-AChRβ antibody (1:100; Abcam, Cambridge, UK), anti-AChRδ antibody (1:5000; Santa Cruz, Santa Cruz, USA), anti-NRG-1 (1:1000; Santa Cruz), anti-ErbB2 (1:1000; Abcam), anti-ErbB3 (1:1000; Abcam), anti-ErbB4 (1:1000; Genetex, Irvine, USA), anti-Akt (1:1000; Cell Signaling Technology), anti-p-Akt (1:1000; Cell Signaling Technology), anti-mTOR (1:1000; Cell Signaling Technology), anti-p-mTOR (1:1000; Cell Signaling Technology), anti-p70S6K (1:1000; Cell Signaling Technology), anti-p-p70S6K (1:1000; Cell Signaling Technology), or anti-β-actin (1:1000; Sigma-Aldrich) at 4°C overnight. After washing, the PVDF membranes were incubated with horseradish peroxidase-conjugated goat anti-rabbit secondary antibody (1:2000; Cell Signaling Technology) or goat anti-mouse secondary antibody (1:2000; Cell Signaling Technology). Finally, protein bands were visualized using scanning densitometer (GS-800; Bio-Rad Laboratories, Hercules, USA) coupled with Bio-Rad personal computer analysis software, and quantified by image J. β-Actin was used as the loading control.

Quantitative real-time PCR

Total RNA was isolated from the IMF and biceps or L6 myoblasts using TRIzol reagent (Invitrogen) according to the manufacturer's protocol. Then, 1 μg of RNA was reverse-transcribed using the PrimeScript RT reagent kit (TaKaRa, Kyoto, Japan). Gene amplification was achieved by real-time PCR using SYBR Green I Mix (Tiangen, Beijing, China) on an ABI Real-Time PCR System (Applied Biosystems, Foster City, USA). The real-time PCR primers are summarized in Table 1. The PCR reactions were carried out using the following settings: one cycle at 95°C for 60 s, 40 cycles of 95°C for 10 s, and 60°C for 30 s, and 72°C for 30 s. The expression of each target gene was calculated using the $2^{-\Delta\Delta CT}$ method. *β-Actin* was used as the housekeeping gene.

Statistical analysis

Data were expressed as the mean ± SEM ($n = 6$) and analysed using SPSS v20.0 software (IBM SPSS, Armonk, USA) and GraphPad Prism 7.0 software (GraphPad Software, San Diego, USA). The data of the OBPP rat model experiments were compared using the Mann-Whitney *U* test. The data in L6 myoblast experiments were compared using Student's *t* test. A *P* value less than 0.05 was considered statistically significant.

Results

Expression levels of NRG-1 and ErbB4 are lower in denervated IMF than in denervated biceps in the OBPP rat model

The expression of NRG-1/ErbB pathway were compared between denervated IMF and denervated biceps in the OBPP rat model, to confirm that the pathway participates in the self-repair of MEPs in denervated skeletal muscles. Relative to the contralateral normal muscles, the protein and mRNA expression levels of NRG-1 ($P < 0.05$ for protein, $P < 0.01$ for mRNA) and ErbB4 ($P < 0.01$) in the denervated IMF were significantly downregulated compared with those of the denervated biceps, but no significant differences were observed in the expressions of ErbB2 and ErbB3 between the two denervated muscles (Figure 1A–C). Laser confocal images showed that 5 weeks after injury, no axonal endings were detected in denervated biceps or IMF; AChR clusters in denervated biceps were still intact, whereas those of denervated IMF were fragmented; ErbB4 receptors appeared diffuse at the postsynaptic membrane in control biceps and IMF; and the density of ErbB4 receptors was lower in denervated biceps, whereas ErbB4 receptors in denervated

Table 1. Sequence of primers used in real-time PCR

Gene	Forward primer (5′→3′)	Reverse primer (5′→3′)
NRG-1	ATCTTCGGCGAGATGTCTGA	TAGCTTGGAGCCTGCAGCTGACT
ErbB2	CCCATCAGAGTGATGTGTGG	TCATCTTCCAGCAGTGAACG
ErbB3	CGTCATGCCAGATACACACC	CTCCTCGTACCCTTGCTCAG
ErbB4	TGGAGGAAAGCCCTATGATG	CTGGGGGACCAAATATTCCT
AChRα	GCCGGACGTTGTTCTCTATAAC	GGTGACAATGATCTCACAGTA
AChRβ	ATGGGAGATTATCCACAAACC	GCAATGACATTGACCAGGTA
AChRδ	CTCGGTCACCTACTTCCCTTTCG	CCGGTGAACTATTTCCCACT
β-actin	AGAGGGAAATCGTGCGTGAC	TAGTGATGACCTGACCGT

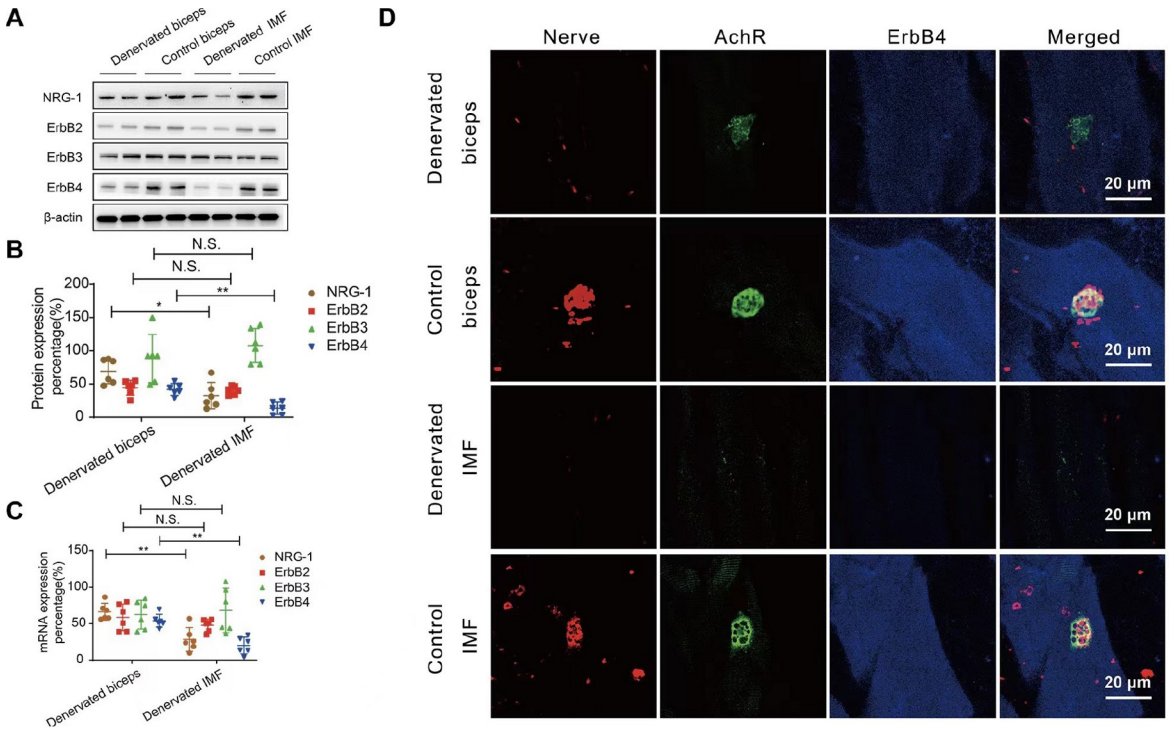

Figure 1. The expression levels of NRG-1 and ErbB4 are lower in denervated IMF than in denervated biceps of the OBPP rat model The protein levels of NRG-1 and ErbB4 were more obviously decreased in denervated IMF than in denervated biceps, whereas those of ErbB2 and ErbB3 were not different between the two groups, as revealed by western blot analysis (A,B). The mRNA levels of NRG-1 and ErbB4 were reduced more significantly in denervated IMF than in denervated biceps, whereas no differences were found in the mRNA levels of ErbB2 and ErbB3 between the two denervated muscles, as revealed by real-time quantitative PCR (C). In representative confocal images (D), the density of ErbB4 protein was decreased in denervated biceps and almost disappeared in denervated IMF. Red: neurofilament; green: α-bungarotoxin; blue: ErbB4. Scale bar: 20 μm. $n = 6$. Denervated IMF *versus* denervated biceps. $^{*}P < 0.05$, $^{**}P < 0.01$. N.S. represents no significance.

IMF almost disappeared (Figure 1D). These data indicated that NRG-1/ErbB4 play an important role in the self-repair of MEPs at the postsynaptic membrane of skeletal muscle following denervation.

NRG-1/ErbB4 have a positive relationship with AChR subunit protein synthesis in L6 myoblasts

To reveal the effects of NRG-1/ErbB4 on AChR synthesis, mRNA and prothein expression levels of AChR subunits were compared between ErbB4-overexpressing and *ErbB4*-knockdown L6 myoblasts. L6 myoblasts were subject to NRG-1 stimulation *in vitro*, and solvent was used as a control. The protein expression levels of AChRα, AChRβ, and AChRδ in the cells treated with NRG-1 were significantly upregulated compared with those treated with solvent (Figure 2A). Next, we used lentivirus to construct a stable ErbB4-overexpressing L6 strain (ErbB4 OV). The protein expression levels of AChRα ($P < 0.01$), AChRβ ($P < 0.01$), and AChRδ ($P < 0.01$) in the ErbB4 OV under NRG-1 stimulation were significantly upregulated compared with those in the vector control (Figure 2B,D). ErbB4 siRNA (si-ErbB4) was used to knock down *ErbB4* in L6 myoblasts, and the results showed that the protein expression levels of AChRα ($P < 0.01$), AChRβ ($P < 0.01$), and AChRδ ($P < 0.01$) in the si-ErbB4 group under NRG-1 stimulation were significantly downregulated compared with thise in the control (NC) group (Figure 2C,E). The mRNA expression levels of AChRα, AChRβ, and AChRδ under NRG-1 stimulation, however, did not differ significantly between the vector and ErbB4 OV groups (Figure 2F) or between the NC and si-ErbB4 groups (Figure 2G). Laser confocal images showed that under NRG-1 stimulation, the density of ErbB4 was higher in the ErbB4 OV group and lower in the si-ErbB4 group relative to their counterparts, and the expression of AChR was upregulated in the ErbB4 OV group and downregulated in the si-ErbB4 group (Figure 2H). These data indicated that NRG-1/ErbB4 have a positive relationship with protein synthesis of AChR subunits instead of mRNA transcription in L6 myoblasts.

Akt plays a role in the positive regulation of AChR subunit protein synthesis by NRG-1/ErbB4 in L6 myoblasts

To identify which downstream signaling molecule takes part in regulating AChR subunit protein synthesis *in vitro*, we inhibited Akt, ERK, and p38 respectively, and measured protein expression of AChR subunits in L6 myoblast. L6 myoblasts were treated with inhibitors of Akt (MK-2206), ERK (PD98059), and p38 (SB203580). When the cells were treated with MK-2206, the protein expression levels of AChRα, AChRβ, and AChRδ showed little change between the vector and ErbB4 OV groups. However, in cells treated with PD98059 or SB203580, a significant increase in the protein expressions of AChRα ($P < 0.01$), AChRβ ($P < 0.01$), and AChRδ ($P < 0.01$) was observed in ErbB4 OV group compared to those in the vector group (Figure 3A–D). AChR expression in laser confocal images was consistent with the western blot analysis results (Figure 3E). These data indicated that Akt is the key downstream signaling molecule of NRG-1/ErbB4 on regulating AChR subunit protein

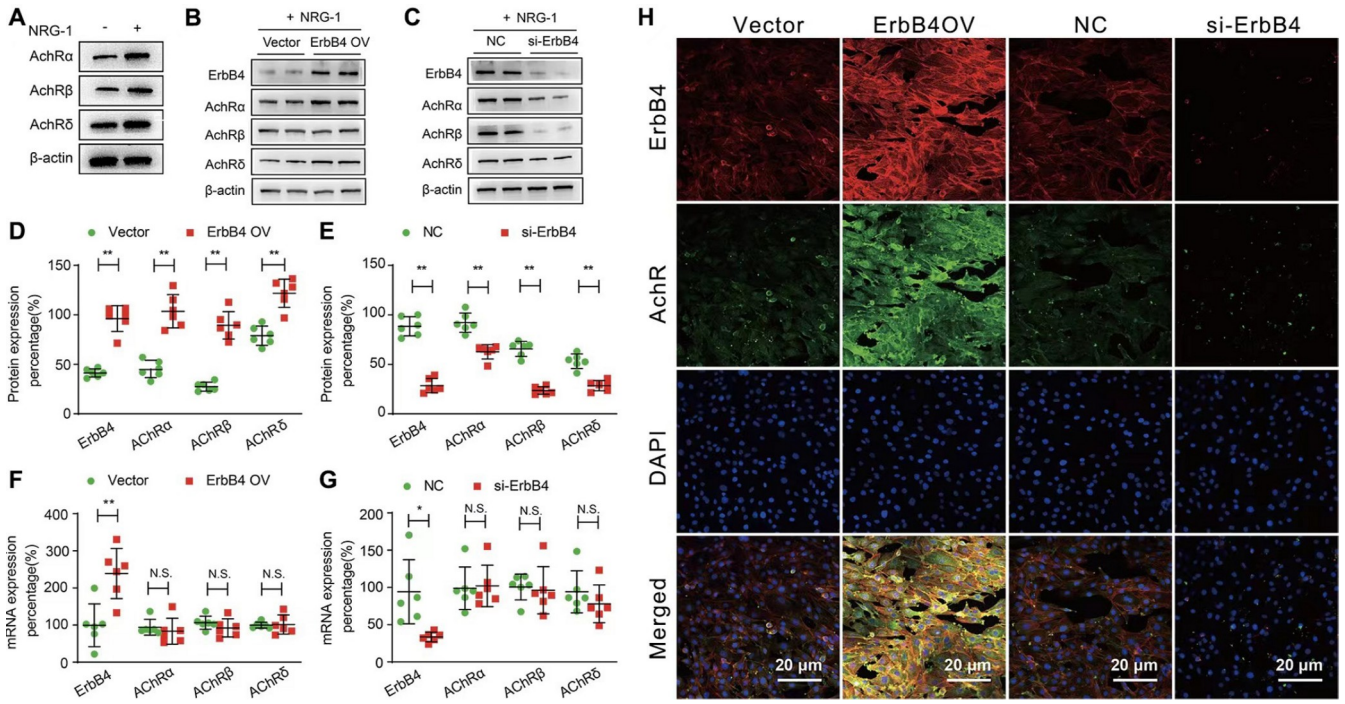

Figure 2. The effects of NRG-1/ErbB4 on regulating the protein synthesis of AChR subunits in L6 myoblasts The protein levels of AChRα, AChRβ, and AChRδ were upregulated in L6 myoblasts treated with NRG-1, as revealed by western blot analysis (A). The protein levels of AChRα, AChRβ, and AChRδ were upregulated in the ErbB4-overexpressing group, as revealed by western blot analysis (B,D). The protein levels of AChRα, AChRβ, and AChRδ were downregulated in L6 myoblasts transfected with ErbB4 siRNA (C, E). The mRNA levels of AChRα, AChRβ, and AChRδ showed no significant changes in ErbB4-overexpressing (F) or *ErbB4*-knockdown (G) L6 myoblasts, as revealed by real-time quantitative PCR. The AChR cluster is upregulated in the ErbB4-overexpressing group and downregulated in the ErbB4-knockdown group in representative confocal images (H). Red: ErbB4; green: α-bungarotoxin; blue: nucleus. Scale bar: 20 μm. $n = 6$. ErbB4 OV *versus* vector, and si-ErbB4 *versus* NC. $^{*}P < 0.05$, $^{**}P < 0.01$. N.S. represents no significance.

synthesis *in vitro*.

Phosphorylation of Akt/mTOR/p70S6K is lower in denervated IMF than in denervated biceps in the OBPP rat model

We compared phosphorylation levels of Akt/mTOR/p70S6K between denervated IMF and denrvated biceps in the OBPP rat model, to verify whether the pathway is involved in the self-repair of MEPs in denervated muscles. In the OBPP rat model, relative to contralateral normal muscles, the protein expression levels of p-Akt ($P < 0.01$), p-mTOR ($P < 0.01$), and p-p70S6K ($P < 0.01$) in the denervated IMF were significantly lower than those in denervated biceps, whereas the protein expression levels of total Akt, mTOR, and p70S6K were not significantly different between the two denervated muscles (Figure 4A–D). Laser confocal images showed that p-mTOR was diffusely distributed at the postsynaptic membrane in normal biceps and normal IMF; the density of p-mTOR in denervated biceps was lower than that in normal biceps, and only little p-mTOR remained in denervated IMF (Figure 4E). These data indicated that phosphorylation levels of Akt/mTOR/p70S6K are down-regulated in denervated IMF relatively, implying a positive relation of activation levels of Akt/mTOR/p70S6K pathway with self-repair of MEPs in denervated muscles.

NRG-1/ErbB4 positively regulates Akt/mTOR/p70S6K phosphorylation in L6 myoblasts

To investigate the relationship between NRG-1/ErbB4 and Akt/mTOR/p70S6K phosphorylation, we measured phosphorylation ratios of Akt, mTOR and p70S6K in ErbB4-overexpressing and *ErbB4*-knockdown L6 myoblasts. Under NRG-1 stimulation of L6 myoblasts, the ratios of p-Akt/Akt ($P < 0.01$), p-mTOR/mTOR ($P < 0.01$), and p-p70S6K/p70S6K ($P < 0.01$) were higher in the ErbB4 OV group and lower in the si-ErbB4 group than in their counterparts (Figure 5A–D). Additionally, when the cells were treated with MK-2206 (an inhibitor of Akt), no significant differences were found in the ratios of p-Akt/Akt, p-mTOR/mTOR, and p-p70S6K/p70S6K between the ErbB4 OV group and the vector group (Figure 5E–H). These data indicated that activation of NRG-1/ErbB4 can up-regulate Akt/mTOR/p70S6K phosphorylation in L6 myoblast, and vice versa.

Inhibition of mTOR abolishes protein synthesis of AChR subunits elevated by NRG-1/ErbB4 in L6 myoblasts

We inhibited mTOR function in ErbB4-overexpressing L6 myoblast to verify whether NRG-1/ErbB4 regulates AChR subunit protein synthesis via Akt/mTOR/p70S6K pathway. In L6 myoblasts under NRG-1 stimulation, treatment with rapamycin (inhibitor of mTOR) led to downregulation of AChRα, AChRβ, AChRδ, p-mTOR and p-p-70S6K expressions in the ErbB4 OV group and vector group (Figure 6A,C). No significant differences were observed in the expression levels of AChRα, AChRβ, and AChRδ or in the ratios of p-mTOR/mTOR and p-p70S6K/p70S6K between the two groups treated with rapamycin (Figure 6B,D). Laser confocal images showed that with rapamycin, AChR clusters almost disappeared in the ErbB4 OV

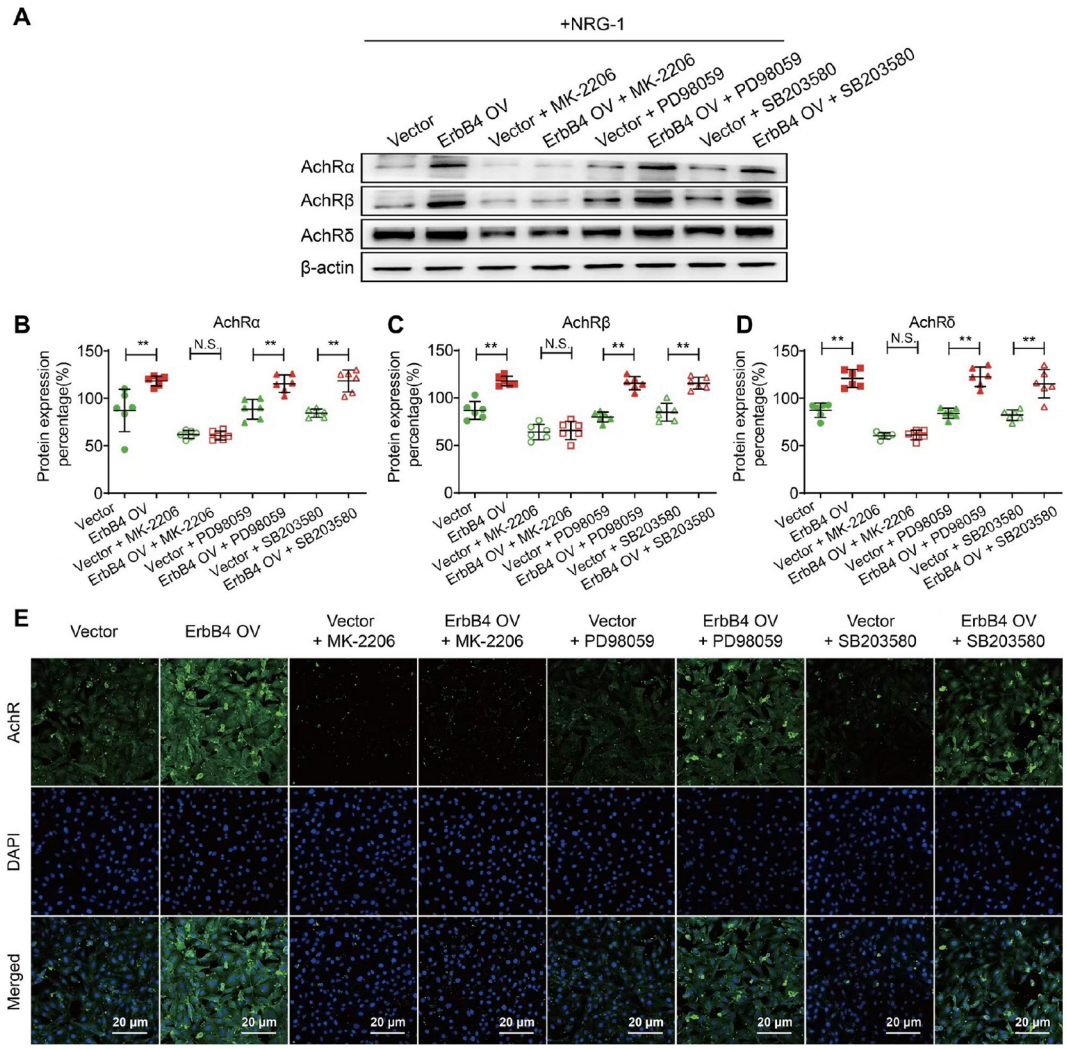

Figure 3. The effects of Akt on regulating the protein synthesis of AChR subunits in L6 myoblasts The ErbB4-induced increases in AChRα, AChRβ, and AChRδ protein levels were blocked in L6 myoblasts treated with MK-2206 (Akt inhibitor) but were not affected by treatment with PD98059 (ERK inhibitor) or SB203580 (p38 inhibitor) (A–D). The AChF cluster is downregulated in vector and ErbB4 OV groups treated with MK-2206, but no changes are observed in either of the groups treated with PD98059 or SB203580 in representative confocal images (E). Green: ErbB4; blue: nucleus. Scale bar: 20 μm. $n = 6$. ErbB4 OV *versus* Vector, ErbB4 OV + MK-2206 *versus* Vector + MK-2206, ErbB4 OV + PD98059 *versus* Vector + PD98059, and ErbB4 OV + SB203580 *versus* Vector + SB203580. $^{**}P < 0.01$. N.S. represents no significance.

group and vector group (Figure 6E). These data indicated that Akt/mTOR/p70S6K is the pivotal downstream signaling pathway of NRG-1/ErbB4 in regulating protein synthesis of AChR subunits.

Discussion

Following peripheral nerve injuries, the loss of innervation leads to degeneration, atrophy, and fibrosis of skeletal muscles [15]. Irreversible atrophy of denervated skeletal muscles is one of the most important factors for functional nonrecovery of peripheral nerves under reconstruction. Clinically, in OBPP, the operative time window of lower trunk injuries is shorter than that of upper trunk injuries [16]. In an OBPP rat model with C5 spinal nerve grafts to the musculocutaneous nerve and C6 to the ulnar nerve, we found that denervated IMF could not regain innervation 5 weeks after injury, whereas denervated biceps could still be reinnervated 10 weeks after injury [4]. These findings indicated that the atrophy of denervated IMH became irreversible more rapidly than that of denervated biceps.

Following denervation, Wallerian degeneration occurs on the distal part of axons, and the postsynaptic membrane begins to degenerate because of the loss of electrochemical stimulation from the presynaptic membrane [17]. In the early stage of denervation, the expression level of AChR is upregulated at the surface of the cytomembrane of skeletal muscles to enhance self-repair of MEPs to improve the ability to adopt regenerated axons. As time passes, however, the expression of AChR falls below the baseline, which leads to the fragmentation of MEPs and results in reduced potential of reinnervation [8,18–20]. In our previous study with an OBPP rat model, MEPs of denervated biceps were found to remain intact morphologically, whereas those of denervated IMF were fragmented; the number and area of MEPs in denervated IMF decreased significantly compared with those in denervated biceps; and the expression levels of AChR α, β, and δ subunits were lower in denervated IMF than in denervated biceps [10]. These findings

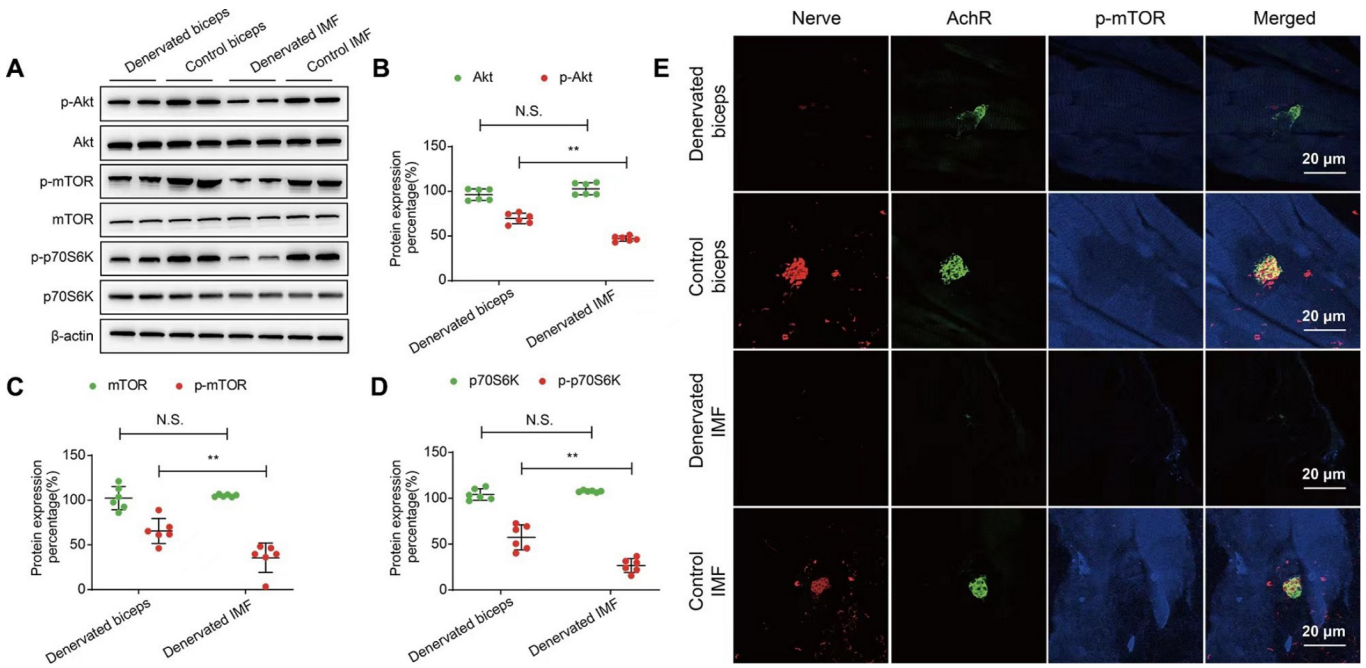

Figure 4. The effects of denervation on the Akt/mTOR/p70S6K signaling pathway in the OBPP rat model The protein levels of p-Akt, p-mTOR, and p-p70S6K were more obviously decreased in denervated IMF than in denervated biceps, but the total Akt, mTOR, and p70S6K protein levels did not show any significant differences (A–D). In representative confocal images (E), the density of p-mTOR is reduced in denervated biceps and almost vanishes in denervated IMF. Red: neurofilament; green: α-bungarotoxin; blue: p-mTOR. Scale bar: 20 μm. $n=6$. Denervated IMF *versus* denervated biceps. $^{**}P<0.01$. N.S. represents no significance.

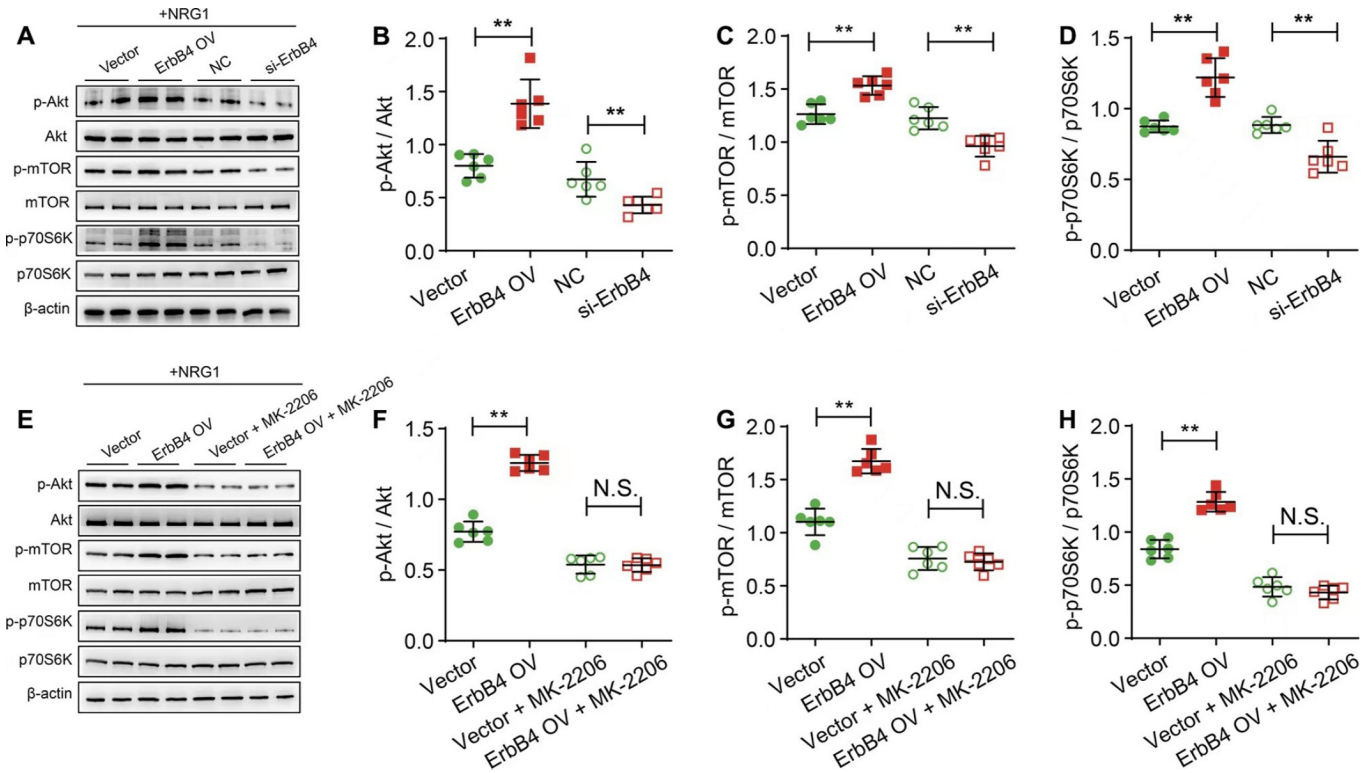

Figure 5. The effects of NRG-1/ErbB4 on positively regulating the phosphorylation of the Akt/mTOR/p70S6K signaling pathway The phosphorylation ratios of p-Akt/Akt, p-mTOR/mTOR, and p-p70S6K/p70S6K were increased in L6 myoblasts that overexpressed ErbB4 and decreased in L6 myoblasts transfected with ErbB4 siRNA (A–D). The effects of ErbB4 on upregulating the phosphorylation ratios of p-Akt/Akt, p-mTOR/mTOR, and p-p70S6K/p70S6K protein levels were blocked in L6 myoblasts overexpressing ErbB4 or vector with MK-2206 treatment (E–H). $n=6$. ErbB4 OV *versus* vector, si-ErbB4 *versus* NC, and ErbB4 OV + MK-2206 *versus* vector + MK-2206. $^{**}P<0.01$. N.S. represents no significance.

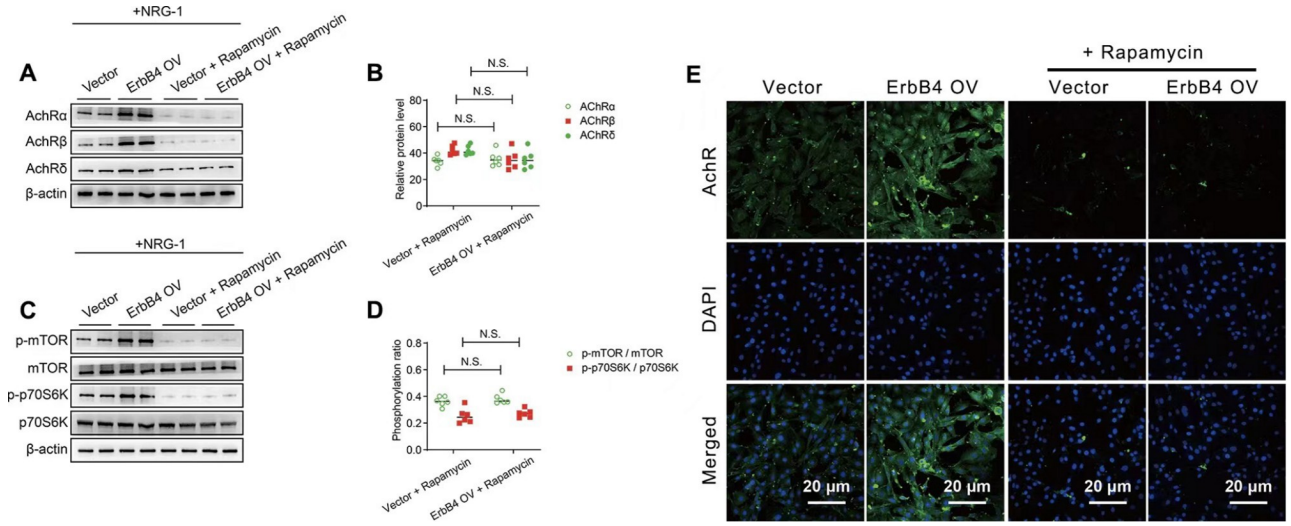

Figure 6. The effects of NRG-1/ErbB4 on regulating the protein synthesis of AChR subunits via mTOR in L6 myoblasts The effects of ErbB4 on increasing AChRα, AChRβ, and AChRδ protein levels are blocked in L6 myoblasts treated with rapamycin (A,B). The effects of ErbB4 on increasing the phosphorylation ratios of p-mTOR/mTOR and p-p70S6K/p70S6K were blocked in L6 myoblasts treated with rapamycin (C,D). AChR clusters are decreased in L6 myoblasts overexpressing ErbB4 and vector with rapamycin treatment in representative confocal images (E). Green: α-bungarotoxin; blue: nucleus. $n = 6$. ErbB4 OV *versus* vector, and ErbB4 OV + rapamycin *versus* vector + rapamycin. $^{**}P < 0.01$. N.S. represents no significance.

indicated that because of the lower expression of AChR subunits, self-repair of MEPs in denervated IMF is worse than that in denervated biceps, which results in reduced potential of reinnervation of the former.

ErbB receptors belong to the epidermal growth factor receptor (EGFR, also called ErbB1) subfamily of the transmembrane tyrosine kinase superfamily, consisting of ErbB2, ErbB3, and ErbB4 subtypes [11]. ErbB receptors are composed of an extracellular domain, a transmembrane domain, a tyrosine kinase domain, and a carboxy-terminal domain [21]. ErbB2 and ErbB4 are specifically expressed on the postsynaptic membrane of NMJs, while ErbB3 is expressed on Schwann cell membrane [11]. As a ligand of ErbB receptors, NRG-1 is an intercellular signal transduction protein synthesized by Schwann cells and neurons. Given that ErbB2 lacks the binding site of NRG-1 and ErbB3 lacks the kinase domain, NRG-1 must bind to the ErbB4 homodimer or ErbB2/3, ErbB2/4, and ErbB1/4 heterodimers to stimulate the tyrosine kinase domain to activate downstream signaling pathways [22]. In the present OBPP rat model, the expression level of ErbB4 was lower in denervated IMF than in denervated biceps, whereas the expression levels of ErbB2 and ErbB3 did not differ significantly between the two muscles. Considering that ErbB4 is located at the postsynaptic membrane of NMJs in skeletal muscles and is an indispensable component of ErbB dimers, our findings indicated that the lack of ErbB4 function may be the reason for the low expression of AChR in denervated IMF.

Muscle spindles, the stretch receptors detecting changes in muscle length, were found in almost all skeletal muscles. The density of muscle spindles was higher in muscles functioning fine with harmonious motions, such as IMH and cervical muscles [23,24]. Barrett *et al.* [25] found that more intrafusal bag myotubes were generated from differentiated C2C12 myoblasts following NRG-1 treatment, suggesting that NRG-1 is indispensable for the development of intrafusal skeletal muscle fibers. These findings highlight the importance of NRG-1 in immature skeletal muscles, especially in fine-functioning ones, during postnatal development. The expression of NRG-1 was much lower in denervated IMF at 5 weeks postinjury, implying that fewer intrafusal skeletal muscle fibers were generated in denervated IMF. Thus, lack of proprioception feedback reestablishment following OBPP might be another reason why satisfactory recovery of IMH function is more difficult to achieve under nerve reconstruction, relative to large muscles of the upper arm.

By interacting with ErbB receptors, NRG-1 participates in the formation of NMJs, innervation and reinnervation in skeletal muscles [26–28]. In our previous study in the OBPP rat model, miR-221 and miR-222 were found to be upregulated in denervated biceps but not changed in denervated IMF at 5 weeks postinjury [5]. Pathway analysis of miRNA expression profiles and recent molecular research [29,30] indicated that these miRNAs participate in the regulation of the NRG-1/ErbB pathway. Thus, the NRG-1/ErbB pathway may play a critical role in regulating the self-repair of MEPs following peripheral nervous injuries. In the present study, we found that overexpression and knockdown of ErbB4 led to increased and decreased protein expression of AChR subunits in L6 myoblasts pretreated with NRG-1, respectively. The results were consistent with other studies in cultured myotubes [31] and *in vivo* [14]. In the present study, we did not observe, however, any variations in mRNA expression, which suggested that the NRG-1/ErbB4 pathway positively regulated protein translation of AChR subunits. These findings imply that in denervated IMF of OBPP, the downregulation of the NRG-1/ErbB4 pathway may decrease protein synthesis of AChR subunits in MEPs, resulting in less self-repair and more severe degeneration of MEPs.

After binding to NRG-1, ErbB receptors dimerize and are autophosphorylated to activate downstream signaling pathways, regulating cell proliferation, differentiation, and apoptosis [32,33]. In the present study, we inhibited Akt, ERK, and p38—several downstream signaling proteins of NRG-1/ErbB4—in L6 myoblasts and found that only Akt is involved in regulating the protein synthesis of AChR subunits. As a serine/threonine protein kinase,

mammalian target of rapamycin (mTOR) is a downstream signal protein of Akt [34]. After being phosphorylated by Akt, active p-mTOR can phosphorylate downstream signal proteins, such as p70 ribosomal S6 kinase (p70S6K) and translation initiation factor elF4E-binding protein 1, to regulate protein translation [35]. We speculated that this is why overexpression of ErbB4 improved the protein expression level but not the mRNA expression level in L6 myoblasts. Therefore, in the OBPP rat model, we examined the expression levels of Akt, mTOR, and p70S6K, and we found that the expression levels of p-Akt, p-mTOR, and p-p70S6K were lower in denervated IMF than in denervated biceps. Furthermore, overexpression of ErbB4 in L6 myoblasts was able to improve the ratios of p-Akt/Akt, p-mTOR/mTOR, and p-p70S6K/p70S6K, thereby confirming that NRG-1/ErbB4 can activate the Akt/mTOR/p70S6K signaling pathway in skeletal muscles.

A number of studies have shown that the Akt/mTOR/p70S6K pathway plays an important role in the proliferation and differentiation of muscle satellite cells [36,37], the formation of nascent muscle fibers [38], and the growth of regenerating muscle fibers during skeletal muscle regeneration [39]. Few studies, however, have focused on its impact on AChR expression in the self-repair of MEPs in skeletal muscles. In this study, we inhibited mTOR in L6 myoblasts and found that ErbB4 overexpression did not upregulate AChR protein synthesis. Thus, we confirmed that NRG-1/ErbB4 could positively regulate AChR protein synthesis through the phosphorylation of the Akt/mTOR/p70S6K pathway in skeletal muscle cells. In our previous study in rats, the mTOR pathway was affected by specific upregulation of miRNA in denervated IMF but not in denervated biceps [5]. Therefore, we inferred that 5 weeks after injury in OBPP, the downregulated expression of NRG-1/ErbB4 leads to less phosphorylation of downstream Akt/mTOR/p70S6K in denervated IMF. This results in regeneration of AChR subunits by limiting their protein translation, consequently exacerbating fragmentation of MEPs and decreasing their ability to adopt regenerative axons, ultimately leading to irreversible atrophy.

In summary, NRG-1/ErbB4 and phosphorylated Akt/mTOR/p70S6K are downregulated more remarkably in denervated IMF than in denervated biceps of the OBPP rat model, and NRG-1/ErbB4 positively regulates AChR protein synthesis in MEPs of skeletal muscle cells through the phosphorylation of the Akt/mTOR/p70S6K signaling pathway. These results indicate that the decline in AChR protein synthesis resulting from the downregulation of NRG-1/ErbB4 is the key molecular mechanism responsible for the rapid atrophy of denervated IMH, which quickly becomes irreversible. NRG-1 has been approved by the US Food and Drug Administration for clinical trials and proven to be tolerable and safe for heart diseases [40,41]. Thus, regulation of the NRG-1/ErbB4 pathway may be a potential treatment option for lengthening the operative window of nerve reconstruction of IMH in OBPP from a translational point of view. Further studies are necessary to assess the effectiveness and safety of NRG-1 delivery in an OBPP rat model.

Funding

This work was supported by the grant from the National Natural Science Foundation of China (No. 81672240 to L.C.).

Conflict of Interest

The authors declare that they have no conflict of interest.

References

1. Davidge KM, Clarke HM, Borschel GH. Nerve transfers in birth related brachial plexus injuries: where do we stand. *Hand Clin* 2016, 32: 175–190
2. Chuang DCC, Mardini S, Ma HS. Surgical strategy for infant obstetrical brachial plexus palsy: experiences at Chang Gung Memorial Hospital. *Plast Reconstr Surg* 2005, 116: 132–142
3. Boome RS. Traumatic branchial plexus injury. In: Gupta A, Kay SPJ, Scheker LR eds. The Growing Hand: Diagnosis and Management of the Upper Extremity in Children. London: Mosby 2000, 653–655
4. Wu J, Chen L, Ding F, Gu Y. A rat model study of atrophy of denervated musculature of the hand being faster than that of denervated muscles of the arm. *J Muscle Res Cell Motil* 2013, 34: 15–22
5. Pan F, Chen L, Ding F, Zhang J, Gu YD. Expression profiles of MiRNAs for intrinsic musculature of the forepaw and biceps in the rat model simulating irreversible muscular atrophy of obstetric brachial plexus palsy. *Gene* 2015, 565: 268–274
6. Wu JX, Chen L, Ding F, Chen LZ, Gu YD. mRNA expression characteristics are different in irreversibly atrophic intrinsic muscles of the forepaw compared with reversibly atrophic biceps in a rat model of obstetric brachial plexus palsy (OBPP). *J Muscle Res Cell Motil* 2016, 37: 17–25
7. Yu XH, Wu JX, Chen L, Gu YD. Inflammation and apoptosis accelerate progression to irreversible atrophy in denervated intrinsic muscles of the hand compared with biceps: proteomic analysis of a rat model of obstetric brachial plexus palsy. *Neural Regen Res* 2020, 15: 1326–1332
8. Zhang BGX, Quigley AF, Bourke JL, Nowell CJ, Myers DE, Choong PFM, Kapsa RMI. Combination of agrin and laminin increase acetylcholine receptor clustering and enhance functional neuromuscular junction formation *in vitro*. *Dev Neurobiol* 2016, 76: 551–565
9. Ma CHE, Omura T, Cobos EJ, Latrémolière A, Ghasemlou N, Brenner GJ, van Veen E, ***et al.*** Accelerating axonal growth promotes motor recovery after peripheral nerve injury in mice. *J Clin Invest* 2011, 121: 4332–4347
10. Li B, Chen L, Gu YD. Stability of motor endplates is greater in the biceps than in the interossei in a rat model of obstetric brachial plexus palsy. *Neural Regen Res* 2020, 15: 1678–1685
11. Trinidad JC, Fischbach GD, Cohen JB. The Agrin/MuSK signaling pathway is spatially segregated from the neuregulin/ErbB receptor signaling pathway at the neuromuscular junction. *J Neurosci* 2000, 20: 8762–8770
12. Ford BD, Liu Y, Anne Mann M, Krauss R, Phillips K, Gan L, Fischbach GD. Neuregulin-1 suppresses muscarinic receptor expression and acetylcholine-activated muscarinic K+ channels in cardiac myocytes. *Biochem Biophys Res Commun* 2003, 308: 23–28
13. Calvo M, Zhu N, Grist J, Ma Z, Loeb JA, Bennett DLH. Following nerve injury neuregulin-1 drives microglial proliferation and neuropathic pain via the MEK/ERK pathway. *Glia* 2011, 59: 554–568
14. Schmidt N, Akaaboune M, Gajendran N, Martinez-Pena y Valenzuela I, Wakefield S, Thurnheer R, Brenner HR. Neuregulin/ErbB regulate neuromuscular junction development by phosphorylation of α-dystrobrevin. *J Cell Biol* 2011, 195: 1171–1184
15. Midrio M. The denervated muscle: facts and hypotheses. A historical review. *Eur J Appl Physiol* 2006, 98: 1–21
16. Chen L, Gu YD, Wang H. Microsurgical reconstruction of obstetric brachial plexus palsy. *Microsurgery* 2008, 28: 108–112
17. Beirowski B, Berek L, Adalbert R, Wagner D, Grumme DS, Addicks K, Ribchester RR, ***et al.*** Quantitative and qualitative analysis of Wallerian degeneration using restricted axonal labelling in YFP-H mice. *J Neurosci Methods* 2004, 134: 23–35
18. Ma J, Shen J, Lee CA, Elsaidi GA, Smith TL, Walker FO, Rushing JT, ***et al.*** Gene expression of nAChR, SNAP-25 and GAP-43 in skeletal muscles

following botulinum toxin A injection: a study in rats. *J Orthop Res* 2005, 23: 302–309
19. Shen J, Ma J, Lee C, Smith BP, Smith TL, Tan KH, Koman LA. How muscles recover from paresis and atrophy after intramuscular injection of botulinum toxin A: study in juvenile rats. *J Orthop Res* 2006, 24: 1128–1135
20. Ma J, Shen J, Garrett JP, Lee CA, Li Z, Elsaidi GA, Ritting A, ***et al.*** Gene expression of myogenic regulatory factors, nicotinic acetylcholine receptor subunits, and GAP-43 in skeletal muscle following denervation in a rat model. *J Orthop Res* 2007, 25: 1498–1505
21. Zhang X, Gureasko J, Shen K, Cole PA, Kuriyan J. An allosteric mechanism for activation of the kinase domain of epidermal growth factor receptor. *Cell* 2006, 125: 1137–1149
22. Weiß FU, Wallasch C, Campiglio M, Issing W, Ullrich A. Distinct characteristics of heregulin signals mediated by HER3 or HER4. *J Cell Physiol* 1997, 173: 187–195
23. Devanandan MS, Ghosh S, John KT. A quantitative study of muscle spindles and tendon organs in some intrinsic muscles of the hand in the bonnet monkey (Macaca radiata). *Anat Rec* 1983, 207: 263–266
24. Cooper S, Daniel PM. Muscle spindles in man; their morphology in the lumbricals and the deep muscles of the neck. *Brain* 1963, 86: 563–586
25. Barrett P, Quick TJ, Mudera V, Player DJ. Neuregulin 1 drives morphological and phenotypical changes in C2C12 myotubes: towards de novo formation of intrafusal fibres in vitro. *Front Cell Dev Biol* 2021, 9: 760260
26. Montero JC, Rodríguez-Barrueco R, Yuste L, Juanes PP, Borges J, Esparís-Ogando A, Pandiella A. The extracellular linker of pro-neuregulin-α2c is required for efficient sorting and juxtacrine function. *Mol Biol Cell* 2007, 18: 380–393
27. Mancuso R, Martínez-Muriana A, Leiva T, Gregorio D, Ariza L, Morell M, Esteban-Pérez J, ***et al.*** Neuregulin-1 promotes functional improvement by enhancing collateral sprouting in SOD1G93A ALS mice and after partial muscle denervation. *Neurobiol Dis* 2016, 95: 168–178
28. Ho BL, Goh Q, Nikolaou S, Hu L, Shay-Winkler K, Cornwall R. NRG/ErbB signaling regulates neonatal muscle growth but not neuromuscular contractures in neonatal brachial plexus injury. *FEBS Lett* 2021, 595: 655–666
29. Puerta-Gil P, García-Baquero R, Jia AY, Ocaña S, Alvarez-Múgica M, Alvarez-Ossorio JL, Cordon-Cardo C, ***et al.*** miR-143, miR-222, and miR-452 are useful as tumor stratification and noninvasive diagnostic biomarkers for bladder cancer. *Am J Pathol* 2012, 180: 1808–1815
30. Feyen E, Ricke-Hoch M, Van Fraeyenhove J, Vermeulen Z, Scherr M, Dugaucquier L, Viereck J, ***et al.*** ERBB4 and multiple microRNAs that target ERBB4 participate in pregnancy-related cardiomyopathy. *Circ Heart Fail* 2021, 14: e006898
31. Ngo ST, Cole RN, Sunn N, Phillips WD, Noakes PG. Neuregulin-1 potentiates agrin-induced acetylcholine receptor clustering through muscle-specific kinase phosphorylation. *J Cell Sci* 2012, 125: 1531
32. Soler C, Beguinot L, Carpenter G. Individual epidermal growth factor receptor autophosphorylation sites do not stringently define association motifs for several SH2-containing proteins. *J Biol Chem* 1994, 269: 12320–12324
33. Lill NL, Sever NI. Where EGF receptors transmit their signals. *Sci Signal* 2012, 5: pe41
34. Swiech L, Perycz M, Malik A, Jaworski J. Role of mTOR in physiology and pathology of the nervous system. *Biochim Biophys Acta* 2008, 1784: 116–132
35. Laplante M, Sabatini DM. mTOR signaling in growth control and disease. *Cell* 2012, 149: 274–293
36. Jash S, Dhar G, Ghosh U, Adhya S. Role of the mTORC1 complex in satellite cell activation by RNA-induced mitochondrial restoration: dual control of cyclin D1 through microRNAs. *Mol Cell Biol* 2014, 34: 3594–3606
37. Rion N, Castets P, Lin S, Enderle L, Reinhard JR, Eickhorst C, Rüegg MA. mTOR controls embryonic and adult myogenesis via mTORC1. *Development* 2019, 146: dev172460
38. Ge Y, Wu AL, Warnes C, Liu J, Zhang C, Kawasome H, Terada N, ***et al.*** mTOR regulates skeletal muscle regeneration in vivo through kinase-dependent and kinase-independent mechanisms. *Am J Physiol Cell Physiol* 2009, 297: C1434–C1444
39. Thomson DM. The role of AMPK in the regulation of skeletal muscle size, hypertrophy, and regeneration. *Int J Mol Sci* 2018, 19: 3125
40. Rupert CE, Coulombe KLK. The roles of neuregulin-1 in cardiac development, homeostasis, and disease. *Biomark Insights* 2015, 10(Suppl 1): 1–9
41. Gao R, Zhang J, Cheng L, Wu X, Dong W, Yang X, Li T, ***et al.*** A phase II, randomized, double-blind, multicenter, based on standard therapy, placebo-controlled study of the efficacy and safety of recombinant human neuregulin-1 in patients with chronic heart failure. *J Am College Cardiol* 2010, 55: 1907–1914